

See discussions, stats, and author profiles for this publication at: <https://www.researchgate.net/publication/256477905>

Photoreduction of CO₂ Using [Ru(bpy)₂(CO)L] (n⁺) Catalysts in Biphasic Solution/Supercritical CO₂ Systems

ARTICLE *in* INORGANIC CHEMISTRY · SEPTEMBER 2013

Impact Factor: 4.76 · DOI: 10.1021/ic401031j · Source: PubMed

CITATIONS

10

READS

32

4 AUTHORS, INCLUDING:



[Patrick Voyame](#)

École Polytechnique Fédérale de Lausanne

5 PUBLICATIONS 46 CITATIONS

[SEE PROFILE](#)



[Kathryn E Toghil](#)

Lancaster University

25 PUBLICATIONS 1,053 CITATIONS

[SEE PROFILE](#)



[Hubert H Girault](#)

École Polytechnique Fédérale de Lausanne

557 PUBLICATIONS 14,009 CITATIONS

[SEE PROFILE](#)

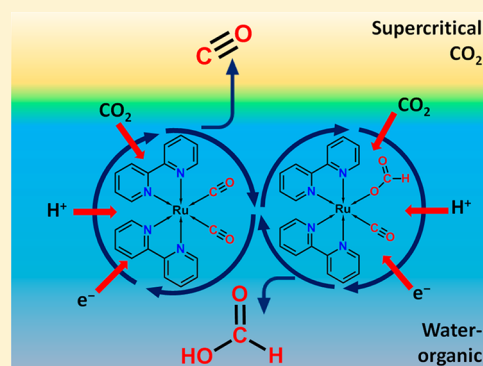
Photoreduction of CO₂ Using [Ru(bpy)₂(CO)L]ⁿ⁺ Catalysts in Biphasic Solution/Supercritical CO₂ Systems

Patrick Voyame, Kathryn E. Toghil, Manuel A. Méndez, and Hubert H. Girault*

Laboratoire Electrochimie Physique et Analytique, Ecole Polytechnique Fédérale de Lausanne, Station 6, CH-1015, Lausanne, Switzerland

Supporting Information

ABSTRACT: The reduction of CO₂ in a biphasic liquid-condensed gas system was investigated as a function of the CO₂ pressure. Using 1-benzyl-1,4-dihydronicotinamide (BNAH) as sacrificial electron donor dissolved in a dimethylformamide–water mixture and [Ru(bpy)₂(CO)L]ⁿ⁺ as a catalyst and [Ru(bpy)₃]²⁺ as a photosensitizer, the reaction was found to produce a mixture of CO and formate, in total about 250 μmol after just 2 h. As CO₂ pressure increases, CO formation is greatly favored, being four times greater than that of formate in aqueous systems. In contrast, formate production was independent of CO₂ pressure, present at about 50 μmol. Using TEOA as a solvent instead of water created a single-phase supercritical system and greatly favored formate synthesis, but similarly increasing CO₂ concentration favored the CO catalytic cycle. Under optimum conditions, a turnover number (TON) of 125 was obtained. Further investigations of the component limits led to an unprecedented TON of over 1000, and an initial turnover frequency (TOF) of 1600 h^{−1}.



INTRODUCTION

During the past decades, the development of artificial photosynthetic systems to harvest solar energy and convert it into a chemical form has increased exponentially.¹ Excess atmospheric levels of CO₂ present a cheap and inexhaustible source of carbon as a starting material to produce chemicals and fuels by its chemical reduction. However, being the final combustion product of every carbon-based fuel and the most oxidized form of carbon, CO₂ has exceptional thermodynamic stability. The direct one-electron reduction to the radical anion CO₂^{•−} is a very unfavorable process.² Other pathways require much less free energy however, and produce considerably more useful products such as methanol and formic acid. These are multielectron proton coupled electron transfer reactions, and reflect the multicomponent steps observed in natural photosynthetic systems.^{1e,3}

Unfortunately, multielectron and proton reactions are kinetically unfavorable, and as such, to compromise between high-energy input and multiple electron transfers, catalysts are required. To achieve multielectron redox reactions, metal complexes are ideal candidates⁴ with metal centers that have variable oxidation states, and interchangeable ligands that can facilitate the reduction of specific molecules, such as CO₂. One class of metal complex catalysts that have been used with considerable success toward CO₂ reduction are bis-bipyridine cationic ruthenium complexes, [Ru(bpy)₂(CO)L]ⁿ⁺ where bpy is 2,2′-bipyridine, L is a hydride or carbonyl ligand (i.e., H, CO₂, C(O)OH, CO), and *n* = 0, 1, or 2. These catalysts, introduced by Tanaka et al.⁵ but also developed by others such as Meyer et al.⁶ and Lehn et al.⁷ are electrochemically active,

and readily react with carbon dioxide to form formic acid and carbon monoxide.

Ruthenium complexes remain one of the most effective homogeneous catalysts for CO₂ reduction, and are still the focus of more recent studies.⁸ Research into alternative metal centers (i.e., osmium,^{6c,9} iridium,¹⁰ rhenium,^{8g,11} and rhodium^{10b,12}) and pyridine based ligands^{8e–g} have proved fruitful, as well as the formation of macro-complexes combining catalyst with photosensitizer^{8a,b} in a single unit.

When photocatalytically reducing CO₂ using [Ru(bpy)₂(CO)H]⁺ as catalyst the reduction products are carbon monoxide and formate, indicating a two electron process. Over the past decades, various mechanisms have been proposed for the reduction process,^{5a,b,6a} and these are summarized in Scheme 1. The key component of metal complexes of this type is the relationship between electron density in the ligand and the metal center. Metal-to-ligand-charge transfer (MLCT) is essential in the coordination of CO₂ to the metal center,^{1d} as the ligands essentially “pool” electrons for subsequent reductions.

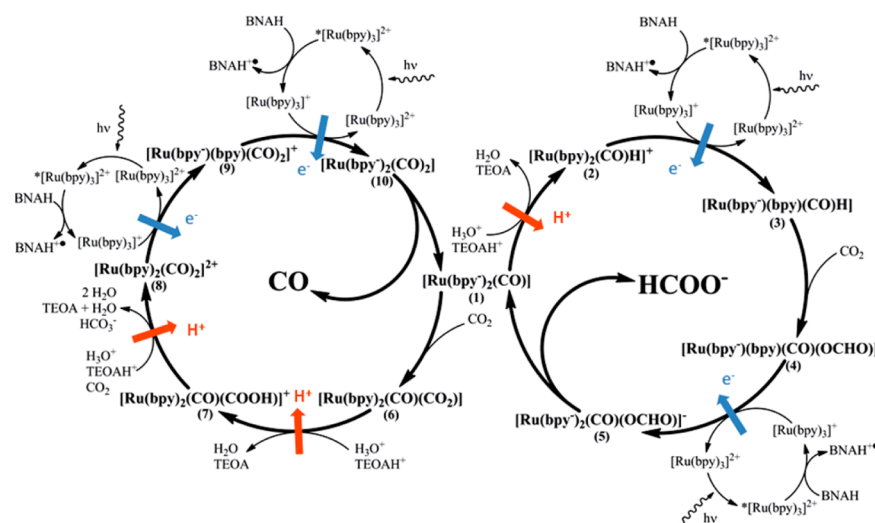
In the case of the catalytic cycle producing carbon monoxide, proposed by Tanaka et al.,^{5a–c,8f} the initial step is the localized reduction of [Ru(bpy)₂(CO)₂]²⁺ (8) at the bpy ligand, occurring at −1.20 V vs saturated calomel electrode (SCE) in aqueous solution. These surplus electrons in the π* orbital of the bipyridyl redistribute across the metal center and the σ* orbital of the Ru–CO bond, thus cleaving the CO molecule

Received: April 25, 2013

Published: September 9, 2013



Scheme 1. Combination of Two Catalytic Cycles for the $[\text{Ru}(\text{bpy})_2(\text{CO})\text{L}]^{n+}$ in the Reduction of CO_2 to Formate or Carbon Monoxide^a



^aThe CO cycle was proposed by Tanaka et al.^{5a} and the formate cycle by Meyer et al.^{6a}

from the complex. In the presence of CO_2 , the now neutral penta-coordinated complex (1) is open to electrophilic attack, resulting in a CO_2 ligand. In aqueous acidic solutions, this complex dehydrates to the starting complex, $[\text{Ru}(\text{bpy})_2(\text{CO})]^{2+}$, completing the catalytic cycle.^{5a,8f} In the absence of water, an organic proton carrier, such as triethanolamine, might be able to protonate the bound CO_2 and induce the release of water. Another possibility is through the formation of bicarbonate from the abstraction of hydroxide by CO_2 (between 7 and 8). Tanaka and co-workers claim that the formation of formate occurs in the equilibration of the three interchangeable species (6–8), but without specific proton attack of the carbon atom, this is debatable. Yet, pH dependence studies by these researchers demonstrated that an alkaline pH favors formate production.^{5a}

Meyer^{6a,9a} proposed an alternative mechanism for the formation of formic acid, based on earlier work by Hawecker et al.¹³ regarding formate formation using only $[\text{Ru}(\text{bpy})_3]^{2+}$ and TEOA in DMF. This second proposed cycle has a common species with the carbon monoxide cycle; $[\text{Ru}(\text{bpy})_2(\text{CO})]^{0+}$ (1). This common intermediate is produced upon reductive elimination of either formate (cycle right) or CO (cycle left). The neutral complex thus produced, being coordinatively unsaturated, contains an available coordination site for a new ligand. The nature of this ligand would seem to dictate the product to be ultimately formed. Hence, CO will be preferentially produced via direct CO_2 coordination, whereas formate predominates when a hydride intermediate is formed instead, followed by CO_2 insertion into the metal-hydride bond.

Conversion of CO_2 to hydrocarbons and oxygenates beyond formic acid and CO is seldom achieved. As the search for even more efficient light or electrochemically driven catalysts continues, another approach to increase CO_2 reduction efficiency is to vastly increase the reactant concentration. Converting CO_2 when it is in a liquid or supercritical state, highly pressurized and highly concentrated, may be a means of maximizing the efficiency of the photocatalysts.

Supercritical CO_2 is a widely used medium for extraction and synthesis,¹⁴ predominantly because of its readily attainable

critical point at the very modest temperature of 31 °C and pressure of just 74 bar. Furthermore, it is relatively inert, nontoxic, and nonflammable. In recent years, a lot of attention has been given to converting supercritical CO_2 to more useful compounds, via electrochemical and photochemical means.¹⁵ It has been dubbed the medium of the future where this application is concerned in a number of recent reviews.^{16,15a} Given that one major limitation in multicomponent photocatalytic systems is that diffusional contact is necessary between the catalyst and reactant, significantly increasing CO_2 concentration can only serve to raise the contact probability.

Hori et al.¹⁶ explored the use of a pressurized system for CO_2 reduction, and demonstrated enhanced catalysis by the rhenium complex, $[\text{fac-ReCl}(\text{bpy})(\text{CO})_3]^+$, by a factor of 5.1 at 25 atm compared to 1 atm,^{16b} with the enhancement in part attributed to the increased stability of the catalyst. In 2011, our group reported the use of nickel cyclam as a catalyst toward CO_2 reduction^{15b} in a scCO_2 -water system. The immiscibility of the two fluids led to an interfacial reaction, in which the catalyst exhibited a much higher turnover for CO_2 reduction relative to the conventional single phase and ambient conditions. In this article, we present a comprehensive study on the influence of CO_2 pressure and concentration on the efficiency and productivity of the well-documented $[\text{Ru}(\text{bpy})_2(\text{CO})(\text{L})]^{n+}$ catalysts.

EXPERIMENTAL SECTION

Materials. Analytical grade dimethylformamide (DMF) (99.99%, Sigma, Switzerland), triethanolamine (TEOA) (99.8%, Sigma, Switzerland), and acetonitrile (Riedel-de Haën, Germany) were used as received. The electron donors, 1-benzyl-1,4-dihydronicotinamide (BNAH) (>95.0%, TCI), triethanolamine and L(+)-ascorbic acid sodium salt (99%, Fluka, Switzerland), photosensitizer, Tris(2,2'-bipyridyl)dichlororuthenium(II) hexahydrate ($\text{Ru}(\text{bpy})_3\text{Cl}_2$) (99.95%, Aldrich, Switzerland), and catalyst precursors RuCl_3 (99.98% metal basis, Aldrich, Switzerland), were also used as received. Deionized water was used throughout the experimental process, prepared using a Milli-Q water system (Milli-Q, resistivity 18.2 MΩ·cm). High purity CO_2 (>99.998%, CarbaGas, Switzerland) was used in all experiments. For the calibration experiments a 500 ppm standard of CO (Carbagas Switzerland) for gas chromatography experiments was used as

received, and sodium formate (99.0%, Fluka, Switzerland) was used for calibration of the ion chromatography.

The catalysts, $[\text{Ru}(\text{bpy})_2(\text{CO}_3)]^+$, $[\text{Ru}(\text{bpy})_2(\text{CO})\text{Cl}]^+$, $[\text{Ru}(\text{bpy})_2(\text{CO})(\text{OCHO})]^+$, and $[\text{Ru}(\text{bpy})_2(\text{CO})\text{H}]^+$ were synthesized in accordance with the procedure outlined by Meyer.^{6c,17}

Equipment. The high-pressure reactor, employed for the photochemical investigation of $[\text{Ru}(\text{bpy})_2(\text{CO})\text{L}]^{n+}$ in high pressure and scCO_2 , was built in-house and comprised a stainless steel cell equipped with a single sapphire window (Rayotek, U.S.A.). The reactor was sealed with a stainless steel cap, which was connected, in series, to two stainless steel autoclaves. The temperature was fixed and controlled by a water circulation system surrounding the reactor, thermostatted externally to $40 \pm 0.2^\circ\text{C}$. The reactor pressure was monitored using a piezoelectric pressure sensor (Swagelok, U.K.). The cell was first filled with the solution containing the electron donor, the photosensitizer, and the catalyst, and CO_2 was introduced and compressed in the reactor using a piston pump (Teledyne Isco, model 100-DX, U.S.A.) until the desired pressure was attained. More details on the experimental setup can be found in the Supporting Information.

The light from a monochromatic high power LED (Thorlabs, M455L2, U.S.A.) (~ 200 mW at 455 nm) irradiated in the reactor during the experimental time (2 h usually), then the reactor was decompressed manually. The gas phase was analyzed by gas chromatography with a methanizer (Clarus 500, PerkinElmer, U.S.A.) and the liquid phase by ion chromatography (Metrohm IC, Switzerland). Details of the ion chromatography procedure can be found in the Supporting Information.

Method. Experiments were conducted in the 32 mL reactor initially filled with 16 mL of a water-DMF liquid phase containing the catalyst $[\text{Ru}(\text{bpy})_2(\text{CO})\text{H}](\text{PF}_6)$, the photosensitizer $[\text{Ru}(\text{bpy})_3]\text{Cl}_2$, and the electron donor. For most of the reactions discussed, the following amounts were used: 2 μmol of the catalyst, 8 μmol of photosensitizer, and 1 mmol of electron donor. The entire system was purged with a gentle flow of CO_2 before the reactor was sealed and compressed to the desired pressure. A sample of the liquid phase was taken to determine the initial concentration of formate present in the solution as contaminant in the solvent used.

The total CO_2 used at each pressure was determined by measuring the volume at low pressure during decompression through the autoclaves. In this mixed system of water-DMF- CO_2 , more CO_2 is contained than if we consider an isolated system of pure CO_2 of equivalent volume, especially below the supercritical pressure. A large amount of CO_2 is evidently dissolved in the solvent, visibly expanding the liquid phase.

RESULTS AND DISCUSSION

Determination of Optimum Experimental Conditions.

To achieve carbon dioxide reduction, electrons and protons must be transferred stepwise to the catalyst (1–10) to form the different products. The advantage of using sacrificial organic electron donors, such as ascorbate, triethanolamine (TEOA), or 1-benzyl-1,4-dihydronicotinamide (BNAH), is that they become very acidic once oxidized and can transfer a proton for each electron they give. From the three aforementioned electron donors, BNAH exhibited the highest productivity by far, and was therefore used in the subsequent experiments.

BNAH is a stronger electron donor than TEOA, but relies on the presence of a proton carrier to transport the proton released from the subsequent chemical reduction, whereas TEOA, because of its weak base nature, is in itself a proton carrier. In Figure 1 two different proton carriers are compared, namely, water and TEOA. The overall production was similar, but the ratio of carbon monoxide/formate differed considerably, as can be seen in Figure 1. Water favors the CO catalytic cycle, whereas TEOA favors the formate cycle (Scheme 1).

Referring back to Scheme 1, at the point of the common intermediate (1), proton or CO_2 addition dictates the path to

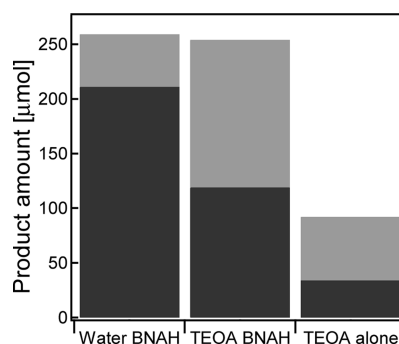


Figure 1. Comparison of the total product formed over 2 h for three systems of varying proton carrier (water or TEOA) and electron donor (BNAH). In dark gray is the total CO formed, and in lighter gray, the total formate. All are in the presence of DMF with 2 μmol catalyst, 8 μmol of photosensitizer, and where applicable, 1 mmol BNAH. The pressure was 150 bar and temperature 313 K.

be followed. If proton addition is slow, addition of CO_2 into the reduced catalyst will be favored, and the main product will then be carbon monoxide.

Under usual conditions, for both water and TEOA with BNAH, the overall amount of product was similar, at about 250 μmol . Thus, control over the proton carrier can provide some control over the selectivity of the product. TEOA can also act as an electron donor; however, it was found that in the absence of BNAH, the productivity of the system greatly decreased, both for formate and for carbon monoxide, with the former still the more abundant (Figure 1).

The composition of the biphasic water-DMF/ scCO_2 system was monitored through the sapphire window of the reactor. Under supercritical conditions, seemingly small changes in the relative composition of the liquid phase strongly affected the reaction conditions and final composition. Without water or with only a small amount (<1 mL), the DMF and CO_2 were completely miscible and a single phase was formed. Increasing the amount of water, but keeping the total volume of the water-DMF phase constant, changes the equilibrium. This led to a biphasic system in which the top phase is pure CO_2 and the bottom phase a CO_2 mixture of DMF/water. In Figure 2, CO and formate productivity is plotted against the water molar fraction in DMF, to ascertain the optimum water to cosolvent

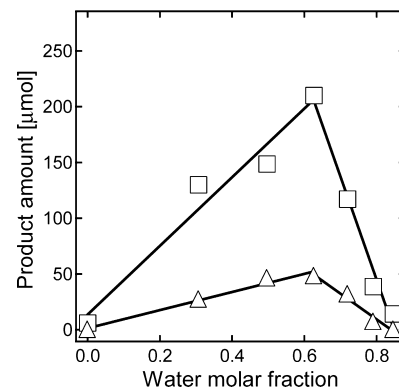


Figure 2. Production of CO (white square) and HCOOH (white triangle) over 2 h as a function of the water molar fraction in DMF. Reaction medium comprises 2 μmol catalyst ($[\text{Ru}(\text{bpy})_2(\text{CO})\text{H}](\text{PF}_6)$), 8 μmol of photosensitizer ($[\text{Ru}(\text{bpy})_3]\text{Cl}_2$), and 1 mmol BNAH. The pressure was 150 bar and temperature 313 K.

ratio. These results were obtained in supercritical CO₂ at 150 bar and 313 K.

It can be seen that production of both carbon monoxide and formate follows the same trend, both reaching a maximum at a water molar fraction of 0.6 (30% water in volume). Without water, no products are formed. In the presence of excess water the catalyst and/or the photosensitizer are less stable, resulting in a sharp decline in productivity. Indeed, the post reaction solutions in the presence of too much or too little water were considerably darker red/orange color than the optimum conditions. Other authors have also reported the instability of the catalyst in high water content conditions.^{6a,7b}

For lower water content (less than 3%, 0.1 mol fraction), the liquid phase expands considerably as the pressure increases to form a single phase. Surprisingly, the single-phase condition is not the most favorable. Achieving a balance between CO₂ concentration and water concentration, explains the product trends in Figure 2. A phase separation is observed to be more favorable to CO production. When TEOA is used as a solvent instead of water only a single phase is observed, regardless of the amount of TEOA.

Effect of CO₂ Pressure. The main objective of this study was to investigate the effect of CO₂ pressure on the response of the system. The reactions used the optimum conditions determined above, with 30% water in volume, BNAH electron donor, the catalyst $[(Ru(bpy)_2(CO)H][PF_6])$, and the photosensitizer $[Ru(bpy)_3](Cl)_2$. The pressure inside the reactor was varied from 10 to 150 bar solely through the addition of pure CO₂. As light penetration into the reactor is very limited because of the high absorbance of the solution, the reaction site is close to the window and far from the liquid/CO₂ interface located at the top of the cell, a few centimeters above the sapphire window.

The effect of CO₂ pressure is shown in Figure 3. The plot overlays the amount of formate, carbon monoxide, and total

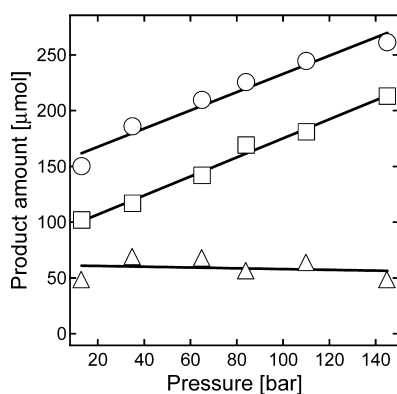


Figure 3. Production of CO (white square), HCOOH (white triangle), and the total amount (white circle) over 2 h in the water-DMF system, as a function of pressure. The molar fraction of water in DMF was 0.6, and the reaction medium consisted of 2 μmol catalyst $[(Ru(bpy)_2(CO)H][PF_6])$, 8 μmol of photosensitizer, and 1 mmol BNAH. The temperature was 313 K.

product formed (CO + HCOO⁻), against pressure. For carbon monoxide, production increased linearly over the pressure range. Overall, carbon monoxide production increased 120% between 10 and 150 bar. The formate yield remained unaffected by CO₂ pressure yielding between 50 and 70 μmol over the pressure range studied. The independence of

formate production on pressure has been noted previously over the 1–10 bar range.^{7b}

These results may be explained by referring to the catalytic cycles in Scheme 1. The most important step dictating whether formate or carbon monoxide will form occurs at the common intermediate (1), the penta-coordinated catalyst awaiting the addition of either H⁺ or CO₂. As CO₂ pressure and concentration increases, the carbon monoxide cycle is favored, as CO₂ is more abundant and forced into the vacant coordination site. This does not account for the steady rate of production of formate that is independent of the CO₂ pressure. Formate synthesis evidently does not compete with CO, as CO increase is greater than formate production, and the latter does not decrease with pressure. In the catalytic scheme, the formate cycle undergoes CO₂ insertion after the first reduction. For the formate cycle, the rate limiting step is probably the electron transfer step (2)–(3) because of the very negative redox potential required to reduce the hydride complex. For the CO cycle CO₂ concentration is involved in the rate limiting step, which can be the oxidative addition of CO₂ (1)–(6) or hydroxide abstraction by proton attack or bicarbonate formation with CO₂.

As shown in Figure 4 when performing the reaction in TEOA/DMF rather than in water/DMF, the overall

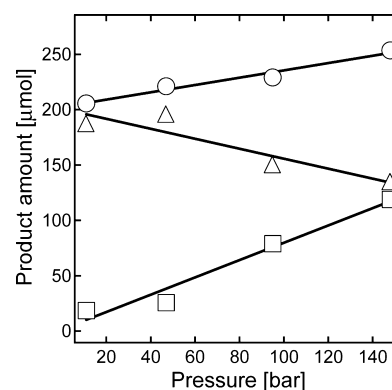


Figure 4. Production of CO (white square), HCOOH (white triangle), and the total amount (white circle) over 2 h in the TEOA-DMF system, as a function of pressure. The TEOA volume fraction was 0.3, and the reaction medium consisted of 2 μmol catalyst, 8 μmol of photosensitizer, and 1 mmol BNAH with a temperature of 313 K.

productivity across the whole pressure range was also 250 μmol. Yet, a significant change in product distribution is depicted, as we observe formate at its highest at 10 bar and 180 μmol, declining to 130 μmol as the pressure is increased. For carbon monoxide however, the initial yield is just 20 μmol at 10 bar, but this increases linearly with pressure until 120 μmol is obtained at 150 bar.

Unlike the water-DMF system, these results show that using TEOA as the proton carrier favors the formate catalytic cycle, and that increasing the CO₂ concentration results in competitive catalysis as the CO₂ is added as a ligand instead of H⁺. The competitive step might therefore be rate-determining for both cycles. Carbon monoxide production is especially favored by the supercritical conditions, as the transition from high pressure to supercritical is met with a 300% increase in CO. Formate concentration decreases somewhat with increasing pressure, suggesting the competition in the catalytic cycles, but may also be due to a detrimental

Table 1. Product Amount, Turnover Number, and Initial Turnover Frequency TOF (h^{-1}) for Different Reaction Conditions^a

	catalyst, μmol	PS, μmol	BNAH, mmol	pressure, bars	light, mW	CO, μmol	TON	TOF _{ini}	HCOOH, μmol	TON	TOF _{ini}
1.	2	8	1	150	200	210	105	78	48	24	35
2.	2	8	1	10	200	103	52	56	48	24	29
3.	0.1	8	1	150	200	102	1020	1120	10	100	480
4.	0.1	8	1	10	200	54	540	280	18	180	360
5.	2	8	1	150	40	80	40	17	59	29.5	9
6.	2	8	2	150	200	193	97	73	91	45	45
7.	2	8	3	150	200	220	110	78	143	72	60
8.	2	0	1	150	200	20	10	ND	10	5	ND
9.	0	8	1	150	200	18	2 ^b	ND	3	0.4 ^b	ND

^aProduct amount (μmol) and TON were calculated after 2 h reactions except for experiment 5, which was a 16 h reaction. ^bCalculated using the photosensitizer amount; ND = not determined.

change in the reaction medium as the reaction components are diluted by the formation of a single phase.

Selectivity in product formation has been suggested in previous publications, with Tanaka et al.^{5a} observing a clear pH dependence on the CO_2 reduction products, with alkaline systems especially favoring the formation of formic acid. More recently, a publication by Tamaki et al.^{8b} noted that the absence of TEOA decreased formate production about 5 fold and also decreased selectivity toward this product. Furthermore HPLC experiments by the authors identified BNAH to be the only contributor as an electron donor. Earlier work by Lehn et al.^{7b} used TEOA as the sole electron donor however, identifying glycoaldehyde and diethanolamine as oxidation products. Here, the TEOA can also donate electrons and quench the excited state, but not sufficiently compared to BNAH as clearly shown in Figure 1.

Turnover Number (TON) and Frequency (TOF) for the Optimized System. The TON is defined as the number of cycles performed by the catalyst in the time scale of the experiment, usually reported when production has reached its limit. It is calculated by dividing the total amount of product, carbon monoxide and formate, by the amount of catalyst in the reactor. The TOF is the number of cycles performed by the catalyst per hour. More generally the initial TOF is reported (TOF_{ini}), which indicates the rate of production at the start of the reaction. This value is calculated from 15 min reactions and is expressed as per hour. Quantum yield (QY) is the ratio of photons converted into electrons to produce the reduction product over the total amount of photons emitted into the reactor (this number is given as a percentage). The total amount of photons absorbed is calculated from the light intensity and reaction time, considering a monochromatic light that is fully absorbed by the solution.

The photocatalytic activity and efficiency of the system under supercritical conditions was determined over a 2 h period. For the two individual systems considered in the previous section, we observed in Figures 3 and 4 that at high pressure and supercritical CO_2 the same total amount of product is reached, about 240 μmol . In water/DMF this corresponded to a TON for the catalyst of 120 in 2 h, and to a TOF_{ini} of 174 h^{-1} (reaction 1 in Table 1). The quantum yield of the reaction, using a monochromatic blue LED, was 9.8%.

These results are difficult to compare to those by Tanaka,^{5b,18} Lehn,¹³ and others^{8a,b} because of the wide variation in reactor volumes, catalytic conditions, reaction time, and light intensity. In the original, and most comparable study by Ishida et al. in 1988,^{18a} the total product after 10 h was 85 μmol , with no more than 30 μmol in the first 2 h. Yet, in

using just 0.5 μmol of catalyst (unlike the 2 μmol used herein), this corresponded to a quantum yield of 14.8% for CO and 2.7% for formate. It is therefore necessary to first identify the limiting factor in the reactions before addressing a comparison of efficiencies in the literature.

Limiting Factors in the Photocatalytic CO_2 Reduction.

Because both the water/DMF and TEOA/DMF reactions reach very similar total productivity, a common limitation is likely to be occurring in both systems. The following sections describe a series of experiments varying catalyst concentration, irradiation time, light intensity, electron donor concentration, and product saturation. For each experiment, unless otherwise stated, the optimized water/DMF system was used for 2 h at an initial pressure of 150 ± 1 bar. The BNAH electron donor concentration was in a large excess at $0.03 \text{ mol}\cdot\text{L}^{-1}$ (1 mmol), the catalyst was $62 \mu\text{mol}\cdot\text{L}^{-1}$ (2 μmol) and the photosensitizer, $[\text{Ru}(\text{bpy})_3]\text{Cl}_2$, was at a concentration of $250 \mu\text{mol}\cdot\text{L}^{-1}$ (8 μmol). The results corresponding to the subsequent variations in parameters are summarized in Table 1, and discussed in the following sections.

Variation in Catalyst Concentration. From the results shown in Figure 5, it can be seen that the amount of catalyst in the reactor can be decreased by a factor of 4 (2 to 0.5 μmol) without any significant modification of the TON. Reducing the amount further however, causes a significant decrease in productivity.

Using the values determined from the smallest added amount of catalyst (result 3 in Table 1), a limiting TON and TOF_{ini} can

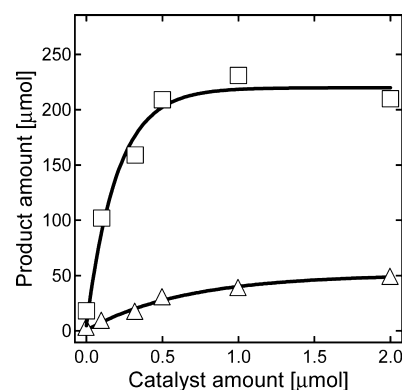


Figure 5. Effect of catalyst ($[(\text{Ru}(\text{bpy})_2(\text{CO})\text{H}][\text{PF}_6])$) concentration on the photocatalytic production of CO (white squares) and HCOO^- (white triangles) over 2 h. The water-DMF system with 1 mmol BNAH and 8 μmol of photosensitizer was used at a pressure of 150 bar and temperature of 313 K.

be estimated. With $0.1 \mu\text{mol}$ of catalyst ($3 \mu\text{mol}\cdot\text{L}^{-1}$), the total amount of product formed is $112 \mu\text{mol}$ in 2 h ($102 \mu\text{mol}$ CO and $10 \mu\text{mol}$ HCOOH). The total TON is therefore 1120, and the TOF_{ini} is 1600 h^{-1} (calculated from the production of $28 \mu\text{mol}$ CO and $12 \mu\text{mol}$ HCOOH in 15 min), values that are considerably larger than the previously mentioned numbers for the optimized volume ratio system. It shows that in the optimum system, the catalytic turnover is not a limiting factor and degradation of the catalyst is not responsible for the limit in total production.

Without catalyst (result 9 in Table 1), a small amount of product is still detected, 18 and $3 \mu\text{mol}$ for CO and HCOOH respectively. This is produced by the conversion of the photosensitizer, $[\text{Ru}(\text{bpy})_3]^{2+}$, into the catalyst unit by the loss of one bipyridyl ligand. The yield is very small compared to that of just $0.1 \mu\text{mol}$ of catalyst however, indicating that photosensitizer degradation is negligible during the 2 h reaction. Other metal carbonyl complexes have been shown to operate catalytically as a single species in the CO_2 reduction cycle.^{7a,9b} Indeed, the catalyst used here can absorb light, and its excited state can be quenched by BNAH to reduce and activate the catalyst. However, the reaction efficiency is limited, as carbon monoxide production decreased 90% from $200 \mu\text{mol}$ to $20 \mu\text{mol}$, and formate production decreased 80% to $10 \mu\text{mol}$. Studies by Tanaka et al. found that the catalytic intermediates (2) and (4) in Scheme 1 are able to excite photolytically at the bpy ligand and accept an electron from the BNAH directly, whereas the double carbonyl ligand intermediates (complexes (8) and (9), Scheme 1) of the carbon monoxide catalytic cycle are not activated by visible light. UV-vis spectroscopy of the catalyst intermediates indicate that the colorless compound $[\text{Ru}(\text{bpy})_2(\text{CO})_2]^{2+}$ is indeed inactive in light above 300 nm wavelength, whereas compounds (2) and (4) of the formate catalytic cycle are bright yellow solids^{2,19} with typical Ru-bpy MLCT absorbance peaks in the blue light region (ca. 450 nm). Control reactions without light did not produce anything.

Performing the experiments at 10 bar with $0.1 \mu\text{mol}$ catalyst (reaction 4 in Table 1) led to a 2-fold decrease in CO yield ($54 \mu\text{mol}$) compared to the experiment at high pressure with the same amount of catalyst (reaction 3). This is a comparable decrease to the high and low pressure experiments with $2 \mu\text{mol}$ catalyst thus maintaining the observation that increasing the pressure to 150 bar doubles CO production. Formate production however is favored at low pressure, and the yield doubled to $18 \mu\text{mol}$, indicating no dependence on CO_2 concentration or pressure but possible competition with CO formation. The total TOF_{ini} at low pressure decreased to 640 h^{-1} (calculated from the production of $7 \mu\text{mol}$ CO and $9 \mu\text{mol}$ HCOOH in 15 min), which corresponds to a 4-fold decrease in CO production rate, and an unchanging rate for HCOOH production when compared to the high-pressure system.

Variation in Irradiation Time and Light Intensity. The results shown in Figure 6 indicate that the reaction is complete after 2 h. Formate production reaches 80% completion in just 30 min, compared to 40% for CO. Reducing light power from 200 to 40 mW reduced the TOF_{ini} proportionally (ca. 5 fold) from 78 to 17 for CO and 36 to 9 for HCOOH. For a lower light intensity experiment the reaction was slower, with the plateau in CO productivity observed after 16 h. The lower intensity was quite detrimental to the final yield for CO, as a TON of 40 was observed compared to 105 in the 200 mW experiment. For HCOOH the final TON was independent of light intensity and remains about 27 ± 3 .

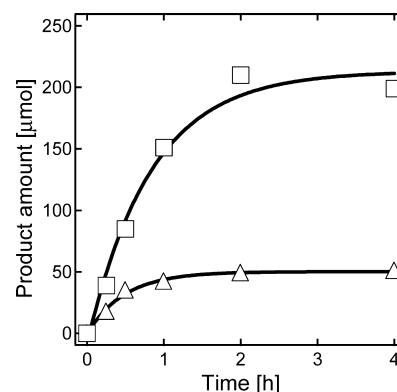
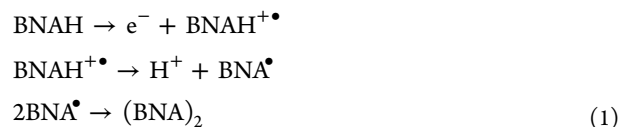


Figure 6. Effect of varying irradiation time on the production of CO (white squares), HCOOH (white triangles). The water-DMF system with 1 mmol BNAH, $2 \mu\text{mol}$ catalyst, and $8 \mu\text{mol}$ of photosensitizer was used at a pressure of 150 bar and temperature of 313 K, light intensity 200 mW.

For a 15-min reaction at 200 mW, the total product yield reaches $57 \mu\text{mol}$, corresponding to a TOF_{ini} of 114 h^{-1} . This TOF is much lower than the previously mentioned limiting TOF for a small amount of catalyst; therefore, one limitation may come from the photosensitization cycle. The irradiation time of 2 h was optimum for the 200 mW reaction, as total productivity reaches a plateau at this time. Considering the shortest irradiation time of 15 min however, the quantum yield is at its highest, with 17.4% of monochromatic light converted to products. A comparable quantum yield of 19.3% was obtained at 40 mW.

Variation in Electron Donor Concentration. Two electrons are necessary for the production of one molecule of carbon monoxide or formate; therefore two molecules of BNAH are required per molecule of product. The electron donor, BNAH, is present in the catalytic system in significant excess to the catalyst and photosensitizer concentrations. Considering that about $250 \mu\text{mol}$ of product is produced in 2 h of reaction with $2 \mu\text{mol}$ of catalyst under 150 bar, about $500 \mu\text{mol}$ of BNAH is consumed, which is 50% of the initial amount. The decrease in BNAH concentration over time might decrease the rate of the photosensitizing cycle, but this does not explain the appearance of a plateau at 50% consumption. The possibility of side reactions and a build up of the oxidation product, BNA_2 , may be a limiting factor in the catalytic cycle. The 1-electron oxidation of BNAH happens through the three following reactions:



An experiment in which the amount of BNAH in the reactor was 1, 2, and 3 mmol was conducted and is shown in Figure 7 and summarized in Table 1 (reactions 1, 6, and 7). At 1 mmol, about $250 \mu\text{mol}$ of total product is obtained. In the reactions with more BNAH however, we observe a trend in which the total CO produced remains at approximately $200 \mu\text{mol}$, yet the formate concentration increases $50 \mu\text{mol}$ (i.e., 100%) per mmol of BNAH. This indicates that the two catalytic cycles undergo two distinct limiting factors that lead to a plateau in the production rate. Carbon monoxide production seems more limited by its own saturation concentration and the formate by

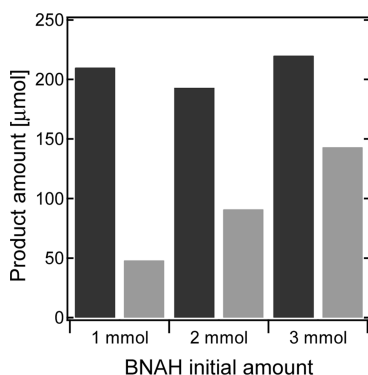


Figure 7. Effect of increasing electron donor concentration on the production of CO (dark gray) and HCOOH (gray) over 2 h. The water-DMF system with 2 μmol catalyst and 8 μmol of $[\text{Ru}(\text{bpy})_3]\text{Cl}_2$ was used at a pressure of 150 bar and temperature of 310 K.

the electron donor concentration. Indeed, the TOF_{ini} for CO production is not influenced at all by the electron donor concentration, but for HCOOH production the TOF_{ini} increases consistently with electron donor concentration. This confirms that the limiting step for CO production involves CO_2 concentration only, presumably the oxidative addition of CO_2 on complex (1) or hydroxide abstraction from CO_2 on complex (7) to form bicarbonate. For HCOOH the limiting step involves the electron donor concentration indicating a limitation in the photosensitizing cycle or in the electron transfer from photosensitizer to the hydride catalyst (2). Indeed, the reduction potential of $[\text{Ru}(\text{bpy})_2(\text{CO})\text{H}]^+$ is 140 mV more negative than $[\text{Ru}(\text{bpy})_3]^{2+}$ (-1.450 and -1.310 V vs SCE respectively),²⁰ indicating an unfavorable electron transfer. This electron transfer will be highly influenced by the concentration of excited state photosensitizer, and therefore influenced by the concentration of the electron donor.

Saturation Interference. For carbon monoxide production, even with a large amount of electron donor (3 mmol) the final concentration does not exceed 220 μmol in the 32 mL reactor used throughout the experiments. It was considered that CO was reaching a saturation concentration, which may have been limiting the reaction by poisoning the catalytic or photosensitization cycles. This was previously reported by Hori et al.^{16a} for a rhenium complex in a high-pressure mixed solvent single phase. To ascertain if the CO was reaching a maximum limit after 2 h and was poisoning the catalyst, the reaction was decompressed at 2-h intervals, the products analyzed, and an additional 1 mmol of BNAH was added to the reactor before recompressing with CO_2 . The results from three consecutive decompressions are shown in Figure 8.

Carbon monoxide ceased to be produced to the same levels (i.e., 200 μmol) after the first 2 h compression, yet the formate was consistently produced at the rate of 50 μmol (± 10 μmol) per compression. This supports that there are two independent cycles occurring to produce the respective products, and they are each limited in different ways.

For carbon monoxide, the theory that a saturating product concentration is poisoning the catalytic cycle is corroborated by this experiment, as production of CO resumes after removing the carbon monoxide produced in the first run. However, production decreased in the two subsequent runs to 135 and 104 μmol for the second and third runs, respectively. A second experiment was then performed in which the gas phase was removed and replenished in the three subsequent reactions, but

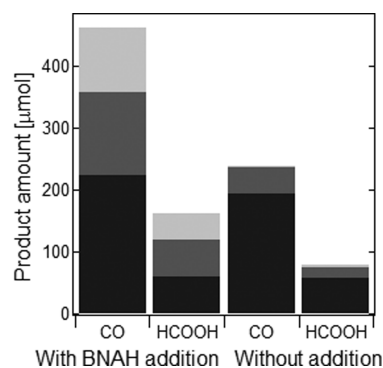
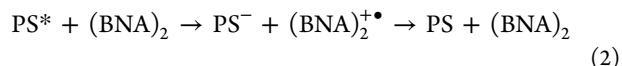


Figure 8. Products formed following periodic 2-h reactions and decompression of the reactor (1st run in dark gray, 2nd in intermediate gray, and 3rd in light gray), with and without addition of 1 mmol of BNAH between runs. The water-DMF system with an initial amount of 1 mmol BNAH, 2 μmol catalyst, and 8 μmol of $[\text{Ru}(\text{bpy})_3]\text{Cl}_2$ was used at a pressure of 150 bar and temperature of 313 K.

further BNAH was not added to the liquid phase. The results shown in Figure 8 strongly indicate the detrimental effect of not replacing the BNAH on CO formation, as productivity decreased to 43 and 2 μmol by the second and third runs, respectively. Formate production was also affected in similar proportions when the electron donor was not replenished.

The dimer BNA_2 is the irreversible product of BNAH oxidation, and it is in itself a very strong reductant, stronger than BNAH ($E_{\text{ox}} = 0.26$ V vs SCE,²¹ $E_{\text{ox}} = 0.57$ V vs SCE²² respectively). With respect to the quenching rate constant published by Tamaki et al., the dimer quenches the excited state of $[\text{Ru}(\text{bpy})_3]^{2+}$ 20 times faster than BNAH. However, unlike for BNAH, the BNA_2 quenching is highly inefficient because of back electron transfer from the photosensitizer to BNA_2 . Finally the BNA_2 is unchanged, but the photosensitizer is no longer excited, as presented in the following



With BNAH as quencher the back electron transfer is certainly hindered by the chemical modification of BNAH^+ induced by the loss of one proton. Because of the increased quenching rate constant of BNA_2 compared to BNAH, as the reaction proceeds, BNAH is converted into BNA_2 , and therefore the quenching is governed by the BNA_2 molecule leading to an inefficient light absorption process. A mathematical model, presented in the Supporting Information, demonstrates the importance of BNA_2 on the efficiency of the photosensitizing cycle. When inefficient quenching by BNA_2 is considered in the model, a noticeable decrease in production rate appears, which corresponds precisely to the production rate observed over 2 h of reaction.

An increase in the initial amount of BNAH in the reactor might reduce the negative effect of the presence of BNA_2 in the reactor. But as shown in Figure 7, the amount of carbon monoxide produced did not change even with 3-fold the initial amount of BNAH in the reactor. The main limitation for carbon monoxide therefore comes from a limiting concentration of products. As pressure increases the concentration of CO_2 in the reactor, the dilution of CO product in the supercritical fluid might explain the improved efficiency of the system at higher pressures.

Formate production increased steadily for the three successive runs in Figure 8, and as such a saturation concentration for this product is excluded but CO saturation seems to limit both catalytic cycles. Another limitation is evidently present because of the limited production of about 50 μmol per run. This may also be due to the increasing concentration of BNA₂ in the reactor. Alternatively, the limited response may be a measure of solution pH, as 50 μmol of formate corresponds to a 3 mM concentration in the water-DMF mixture (though solvent expansion dilutes this somewhat), with the additional decrease in pH corresponding to the dissolution of CO₂ to carbonic acid. This would further explain the decrease in formate production at higher CO₂ concentrations, as undoubtedly the solution will have a lower pH. The solution pH has been determined to be highly influential on product formation in this catalytic system by earlier work,²³ and therefore must not be discounted from the explanations.

CONCLUSIONS

The effects of increased CO₂ pressure and imparting supercritical conditions on the catalytic reaction of the well characterized CO₂ reduction catalyst [Ru(bpy)₂(CO)(H)]⁺ have been presented. CO₂ reduction was comprehensively optimized with respect to proton carrier, cosolvent, and CO₂ concentration/pressure, providing further insight into the catalytic cycles, the relationship between catalyst, photosensitizer, and electron donor, and demonstrating the advantages of vastly increasing CO₂ concentration on the catalytic system.

The two products identified in the analysis were carbon monoxide and formate. The former was found to have a linear relationship with pressure over a 10–150 bar range, such that production was consistently doubled. Formate, however, was independent of CO₂ concentration in water/DMF solutions, and decreased 25% in a TEOA/DMF medium between 10 and 150 bar. Increasing CO₂ concentration therefore favors the CO catalytic cycle and is rate limiting for the reaction, whereas formate is independent of CO₂ concentration because of insertion later in the catalytic cycle. It was found that the greatest CO yields were obtained from a biphasic water/DMF supercritical CO₂ system rather than a single phase of all components. This was suggested to be due to the extraction of CO from the liquid water phase where the catalyst was present to the upper condensed/supercritical CO₂ phase, thus preventing the catalytic cycle from being poisoned. Nonetheless, a saturation concentration of about 200 μmol was identified in subsequent experiments at optimum conditions.

TONs and TOFs for the optimized systems were considerably greater than previously reported in the literature.^{5b,7b,8b,18} For a system irradiated for 2 h with 2 μmol of catalyst, the TON was 120 with a TOF_{ini} of 174 h⁻¹, but this reached 1120 h⁻¹ and 1600 h⁻¹ when the catalyst was used at its limit of 0.1 μmol . The rapid turnover and overall productivity of the systems compared to the literature demonstrates the enhancement offered by operating the reaction at high-pressure over the range of 10–150 bar, and the potential for obtaining much more product in a short time frame. Work is underway to further elucidate the catalytic cycles by electrochemistry and coupled mass spectrometry.

ASSOCIATED CONTENT

Supporting Information

Further information on the high pressure setup, ion chromatography procedure, choice of catalyst, electron donor and proton carrier, and mathematical kinetic model of the electron donor quenching mechanism. This material is available free of charge via the Internet at <http://pubs.acs.org>.

AUTHOR INFORMATION

Corresponding Author

*E-mail: hubert.girault@epfl.ch. Fax: +41 (0)21 693 36 67. Phone: +41 (0)21 693 31 51.

Notes

The authors declare no competing financial interest.

ACKNOWLEDGMENTS

P.V. would like to thank the Swiss National Science Foundation (SNSF) for financial support. We also acknowledge financial support from Poleswiss PSPB-035/2010.

REFERENCES

- (1) (a) Song, W.; Chen, Z.; Brennaman, M. K.; Concepcion, J. J.; Patrocinio, A. O. T.; Iha, N. Y. M.; Meyer, T. J. *Pure Appl. Chem.* **2011**, *83* (4), 749–768. (b) Alstrum-Acevedo, J. H.; Brennaman, M. K.; Meyer, T. J. *Inorg. Chem.* **2005**, *44* (20), 6802–6827. (c) Willner, I.; Willner, B. *Top. Curr. Chem.* **1991**, *159* (Photoinduced Electron Transfer 3), 153–218. (d) Concepcion, J. J.; House, R. L.; Papanikolas, J. M.; Meyer, T. J. *Proc. Natl. Acad. Sci.* **2012**, *109* (39), 15560–15564. (e) Meyer, T. J. *Acc. Chem. Res.* **1989**, *22* (5), 163–170. (f) Grills, D. C.; Fujita, E. *J. Phys. Chem. Lett.* **2010**, *1* (18), 2709–2718.
- (2) Tanaka, K.; Ooyama, D. *Coord. Chem. Rev.* **2002**, *226* (1–2), 211–218.
- (3) Gagliardi, C. J.; Westlake, B. C.; Kent, C. A.; Paul, J. J.; Papanikolas, J. M.; Meyer, T. J. *Coord. Chem. Rev.* **2010**, *254* (21–22), 2459–2471.
- (4) Fujita, E. *Coord. Chem. Rev.* **1999**, *185*–186, 373–384.
- (5) (a) Ishida, H.; Tanaka, K.; Tanaka, T. *Organometallics* **1987**, *6* (1), 181–186. (b) Ishida, H.; Tanaka, K.; Tanaka, T. *Chem. Lett.* **1987**, *6*, 1035–1038. (c) Ishida, H.; Tanaka, H.; Tanaka, K.; Tanaka, T. *J. Chem. Soc., Chem. Commun.* **1987**, *2*, 131–132. (d) Tanaka, K.; Morimoto, M.; Tanaka, T. *Chem. Lett.* **1983**, *6*, 901–904.
- (6) (a) Pugh, J. R.; Bruce, M. R. M.; Sullivan, B. P.; Meyer, T. J. *Inorg. Chem.* **1991**, *30* (1), 86–91. (b) Sullivan, B. P.; Meyer, T. J. *J. Chem. Soc., Chem. Commun.* **1984**, *18*, 1244–1245. (c) Sullivan, B. P.; Caspar, J. V.; Meyer, T. J. *Organometallics* **1984**, *3* (8), 1241–1251.
- (7) (a) Hawecker, J.; Lehn, J. M.; Ziessel, R. *Helv. Chim. Acta* **1986**, *69* (8), 1990–2012. (b) Lehn, J. M.; Ziessel, R. *J. Organomet. Chem.* **1990**, *382* (1–2), 157–173.
- (8) (a) Tamaki, Y.; Watanabe, K.; Koike, K.; Inoue, H.; Morimoto, T.; Ishitani, O. *Faraday Discuss.* **2012**, *155*, 115–127. (b) Tamaki, Y.; Morimoto, T.; Koike, K.; Ishitani, O. *Proc. Natl. Acad. Sci. U. S. A.* **2012**, *109*, 15673–15678, S15673/1–S15673/7. (c) Ohtsu, H.; Tanaka, K. *Angew. Chem., Int. Ed.* **2012**, *51* (39), 9792–9795, S9792/1–S9792/10. (d) Chen, Z.; Chen, C.; Weinberg, D. R.; Kang, P.; Concepcion, J. J.; Harrison, D. P.; Brookhart, M. S.; Meyer, T. J. *Chem. Commun. (Cambridge, U. K.)* **2011**, *47* (47), 12607–12609. (e) Tsukahara, Y.; Wada, T.; Tanaka, K. *Chem. Lett.* **2010**, *39* (11), 1134–1135. (f) Tanaka, K. *Chem. Rec.* **2009**, *9* (3), 169–186. (g) Fujita, E.; Muckerman, J. T.; Tanaka, K. *Prepr. Symp. - Am. Chem. Soc., Div. Fuel Chem.* **2008**, *53* (1), 238–239.
- (9) (a) Bruce, M. R. M.; Megehee, E.; Sullivan, B. P.; Thorp, H. H.; O'Toole, T. R.; Downard, A.; Pugh, J. R.; Meyer, T. J. *Inorg. Chem.* **1992**, *31* (23), 4864–4873. (b) Chauvin, J.; Lafalet, F.; Chardon-Noblat, S.; Deronzier, A.; Jakonen, M.; Haukka, M. *Chem.—Eur. J.* **2011**, *17* (15), 4313–4322.

- (10) (a) Rasmussen, S. C.; Richter, M. M.; Yi, E.; Place, H.; Brewer, K. J. *Inorg. Chem.* **1990**, *29* (20), 3926–3932. (b) Bolinger, C. M.; Story, N.; Sullivan, B. P.; Meyer, T. J. *Inorg. Chem.* **1988**, *27* (25), 4582–4587.
- (11) (a) Johnson, F. P. A.; George, M. W.; Hartl, F.; Turner, J. J. *Organometallics* **1996**, *15* (15), 3374–3387. (b) Sullivan, B. P.; Bolinger, C. M.; Conrad, D.; Vining, W. J.; Meyer, T. J. *J. Chem. Soc., Chem. Commun.* **1985**, *20*, 1414–1416. (c) Hawecker, J.; Lehn, J. M.; Ziessel, R. *J. Chem. Soc., Chem. Commun.* **1984**, *6*, 328–330.
- (12) (a) Szymaszek, A.; Pruchnik, F. P. *J. Organomet. Chem.* **1989**, *376* (1), 133–140. (b) Bolinger, C. M.; Sullivan, B. P.; Conrad, D.; Gilbert, J. A.; Story, N.; Meyer, T. J. *J. Chem. Soc., Chem. Commun.* **1985**, *12*, 796–797.
- (13) Hawecker, J.; Lehn, J.-M.; Ziessel, R. *J. Chem. Soc., Chem. Commun.* **1985**, *2*, 56–58.
- (14) Beckman, E. J. *J. Supercrit. Fluids* **2004**, *28* (2–3), 121–191.
- (15) (a) Doherty, M. D.; Grills, D. C.; Muckerman, J. T.; Polyansky, D. E.; Fujita, E. *Coord. Chem. Rev.* **2010**, *254* (21–22), 2472–2482. (b) Méndez, M. A.; Voyame, P.; Girault, H. H. *Angew. Chem., Int. Ed.* **2011**, *50* (32), 7391–7394.
- (16) (a) Hori, H.; Koike, K.; Suzuki, Y.; Ishizuka, M.; Tanaka, J.; Takeuchi, K.; Sasaki, Y. *J. Mol. Catal. A: Chem.* **2002**, *179* (1–2), 1–9. (b) Hori, H.; Takano, Y.; Koike, K.; Sasaki, Y. *Inorg. Chem. Commun.* **2003**, *6* (3), 300–303.
- (17) Johnson, E. C.; Sullivan, B. P.; Salmon, D. J.; Adeyemi, S. A.; Meyer, T. J. *Inorg. Chem.* **1978**, *17* (8), 2211–2215.
- (18) (a) Ishida, H.; Tanaka, K.; Tanaka, T. *Chem. Lett.* **1988**, *2*, 339–42. (b) Ishida, H.; Terada, T.; Tanaka, K.; Tanaka, T. *Inorg. Chem.* **1990**, *29* (5), 905–911.
- (19) Ooyama, D.; Tomon, T.; Tsuge, K.; Tanaka, K. *J. Organomet. Chem.* **2001**, *619* (2), 299–304.
- (20) Juris, A.; Balzani, V.; Barigelletti, F.; Campagna, S.; Belser, P.; von Zelewsky, A. *Coord. Chem. Rev.* **1988**, *84* (0), 85–277.
- (21) Patz, M.; Kuwahara, Y.; Suenobu, T.; Fukuzumi, S. *Chem. Lett.* **1997**, *6*, 567–568.
- (22) Fukuzumi, S.; Koumitsu, S.; Hironaka, K.; Tanaka, T. *J. Am. Chem. Soc.* **1987**, *109* (2), 305–316.
- (23) Ishida, H.; Tanaka, K.; Morimoto, M.; Tanaka, T. *Organometallics* **1986**, *5* (4), 724–730.